ISSN 1674-1056
http://cpb.iphy.ac.cn
http://iopscience.iop.org/cpb
中国物理 B
Chinese Physics
中国物理 Chinese Physics B

Third-order nonlinear optical properties of graphene composites: A review

Meng Shang(尚萌), Pei-Ling Li(李培玲), Yu-Hua Wang(王玉华), and Jing-Wei Luo(罗经纬)
Citation: Chin. Phys. B, 2021, 30 (**8**): 080703. DOI: 10.1088/1674-1056/ac0424
Journal homepage: http://cpb.iphy.ac.cn; http://iopscience.iop.org/cpb

What follows is a list of articles you may be interested in

Optical sensors based on the NiPc–CoPc composite films deposited by drop casting and under the action of centrifugal force

Noshin Fatima, Muhammad M Ahmed, Khasan S Karimov, Zubair Ahmad, Fahmi Fariq Muhammad
Chin. Phys. B, 2017, 26 (**6**): 060704. DOI: 10.1088/1674-1056/26/6/060704

Ultralow detection limit of giant magnetoresistance biosensor using Fe_3O_4-graphene composite nanoparticle label

Jie Xu(徐洁), Ji-qing Jiao(焦吉庆), Qiang Li(李强), Shan-dong Li(李山东)
Chin. Phys. B, 2017, 26 (**1**): 010701. DOI: 10.1088/1674-1056/26/1/010701

Experimental research on spectrum and imaging of continuous-wave terahertz radiation based on interferometry

Tie-Lin Lu(卢铁林), Hui Yuan(袁 慧), Ling-Qin Kong(孔令琴), Yue-Jin Zhao(赵跃进), Liang-Liang Zhang(张亮亮), Cun-Lin Zhang(张存林)
Chin. Phys. B, 2016, 25 (**8**): 080702. DOI: 10.1088/1674-1056/25/8/080702

Preparation and room temperature NO_2-sensing performances of porous silicon/V_2O_5 nanorods

Wen-Jun Yan(闫文君), Ming Hu(胡明), Ji-Ran Liang(梁继然), Deng-Feng Wang(王登峰), Yu-Long Wei(魏玉龙), Yu-Xiang Qin(秦玉香)
Chin. Phys. B, 2016, 25 (**4**): 040702. DOI: 10.1088/1674-1056/25/4/040702

Computer simulation of the bombardment of a copper film on graphene with argon clusters

A. Y. Galashev, O. R. Rakhmanova
Chin. Phys. B, 2015, 24 (**2**): 020701. DOI: 10.1088/1674-1056/24/2/020701

REVIEW

Third-order nonlinear optical properties of graphene composites: A review*

Meng Shang(尚萌)†, Pei-Ling Li(李培玲)†, Yu-Hua Wang(王玉华)‡, and Jing-Wei Luo(罗经纬)

Hubei Province Key Laboratory of Science in Metallurgical Process, Wuhan University of Science and Technology, Wuhan 430081 *China*

(Received 23 March 2021; revised manuscript received 18 April 2021; accepted manuscript online 24 May 2021)

Graphene has excellent thirdorder nonlinear optical (NLO) properties due to its unique electronic band structure and wideband gap tunability. This paper focuses on the research progress of graphene and its composite materials in nonlinear optics in recent years. In this review, recent results on graphene (or graphene oxide)–metal nanoparticles (G-MNPs), graphene–metal–oxide nanoparticles (G-MONPs), graphene–metal sulfide nanoparticles (G-MSNPs), and graphene–organic molecular composites (G-OM) have been discussed. In addition, the enhancement mechanism of nonlinear absorption (NLA) and optical limiting (OL) have also been covered.

Keywords: graphene, composites, nonlinear optics, optical limiting, enhancement

PACS: 07.60.–j **DOI:** 10.1088/1674-1056/ac0424

1. Introduction

1.1. Theory of nonlinear optics

Before the laser was invented, most of the research was about the propagation of low light in the medium. It was believed that the polarization index of the refractive index of the material was constant, independent of the light intensity, material intensity, and polarization that increased with the increase of the laser intensity. The photoelectric field E follows the principle of superposition of linear light waves. But the relationship between polarization intensity and incident light amplitude is no longer linear.[1–4] Rather, it is related to the second, third, and even higher order of field intensity, that is, optical nonlinearity. On the one hand, the light field magnetizes and polarizes the material and generates an induced current. So that the material produces electromagnetic field radiation. On the other hand, the electromagnetic field radiation generated by the matter will in turn affect the original light field at the same time.[5–8]

During the period from 1961 to 1965, since the advent of the laser, Franken accidentally discovered the frequency doubling effect in the ruby laser in the experiment, thus opening the door to a new field. Subsequently, a series of nonlinear optical phenomena were discovered: sum frequency (SF), difference frequency (DF), parametric oscillation (PO), four-wave mixing (FWM), saturation absorption (SA), and reverse saturation absorption (RSA), *etc*.[9] From 1965 to 1969, the main phenomena discovered were: transient coherent optical (TCO) effects, self-focusing (SF) effects, photo-induced breakdown (PB) effects, phase conjugation (PC) effects, and self-phase modulation (SPM) effects. Since the 1970s, the research objects of nonlinear optics have gradually expanded. For example: from the research of compounds to the research of various composite materials. From the third-order nonlinear effect to the development of higher-order research; from the research of bulk materials The development of two-dimensional or even one-dimensional materials.[10,11]

For isotropic media, the vector P of nonlinear polarization can be rewritten into the following form:

$$P = \varepsilon_0\chi^{(1)}E + \varepsilon_0\chi^{(2)}EE + \varepsilon_0\chi^{(3)}EEE + \cdots, \quad (1a)$$

$$P = P_{\rm L} + P_{\rm NL}, \quad (1b)$$

$$P_{\rm L} = \varepsilon_0\chi^{(1)}E, \quad (1c)$$

$$P_{\rm NL} = \varepsilon_0\chi^{(2)}EE + \varepsilon_0\chi^{(3)}EEE + \cdots. \quad (1d)$$

Equations (1a), (1b), and (1c) are the first-order linear polarizability, second-order nonlinear polarizability, and third-order nonlinear polarizability of the medium. There are two main reasons for the third-order nonlinear polarizability: component polarization and structural polarization. Among them, the chemical composition change caused by light belongs to the external change of the substance, mainly due to the optical nonlinearity caused by the chemical reaction of light. Structural refers to light-induced changes in the internal structure of atoms or molecules, such as molecular steering, mean free path, and electron number density. These changes all originate from the internal structure of the substance.[12]

*Project supported by the National Natural Science Foundation of China (Grant No. 11375136).

†The authors contributed equally to this work.

‡Corresponding author. E-mail: wangyuhua@wust.edu.cn

© 2021 Chinese Physical Society and IOP Publishing Ltd

1.2. The *Z*-scan technique

The first time *Z*-scan theory technology was proposed by researchers such as Sheik Bahae.[13,14] The experimental equipment is shown in Fig. 1. When the Gaussian beam emitted by the laser passes through the attenuator A and reaches the beam splitter BS, part of the light will be incident on the detector D_2 for reference data. The other part of the light will continue to propagate in the positive direction of the Z axis and be focused by the convex lens. The tester can control the movement of the substance to be measured on the Z axis, measure the transmittance corresponding to each position, and then obtain the Z scan test data. Through the Z scan curve, the sign of the nonlinear refractive index of the sample can also be obtained. When the T–Z curve shows a peak before a valley, the nonlinear coefficient of the material is negative. Conversely, when the T–Z curve shows a valley before a peak, the nonlinear coefficient of the material is positive.[15,16]

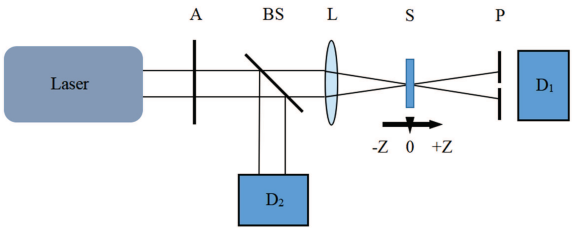


Fig. 1. Schematic diagram of the optical path of the Z-scan equipment. BS: beam splitter; L: lens; S: sample; D1, D2: detector.

1.3. Nonlinear optical parameters

The theoretical curve of the normalized transmittance of Z-scan can be expressed as[18]

$$T(z) = 1 - \frac{4 \cdot x \cdot \Delta\Phi_0}{(x^2+1)\cdot(x^2+9)}, \tag{2}$$

where $\Delta\Phi_0$ is the phase shift at the focus. $x = z/z_0$, z_0 is the Rayleigh length of the beam. The total absorption coefficient α can be obtained by using the following equation:

$$\alpha(I) = \frac{\alpha_0}{1 + I/I_s} + \beta_{\text{eff}} \cdot I. \tag{3}$$

Here, β_{eff} is the nonlinear absorption coefficient, I is the on-axis peak irradiance, α is the linear absorption coefficient, and I_s is the saturation irradiance.[19,20] The nonlinear refractive index n_2 (cm^2/GW) is obtained from the best fitting performed on the experimental data by

$$n_2 = \frac{\Delta\Phi_0}{K \cdot L_{\text{eff}} \cdot I_0}. \tag{4}$$

The third-order nonlinear refractive index γ can be expressed as

$$\gamma = \frac{\lambda \cdot \Delta\Phi_0}{2 \cdot \pi \cdot I_0 \cdot L_{\text{eff}}}. \tag{5}$$

2. Third-order nonlinear optical effect

2.1. Nonlinear refraction mechanisms

Studies have shown that nonlinear materials interact with incident light under the influence of intense laser light. Many physical mechanisms inside the material can cause changes in the refraction of the medium. The response time of these change mechanisms is different from the corresponding principles. The contribution of different response mechanisms is related to the pulse duration of the laser light source. The real part of the material's third-order nonlinear polarizability $\chi^{(3)}$ represents the nonlinear refraction. In general, the physical mechanisms that produce nonlinear refraction changes include the following: electronic cloud distortion, nuclear movement, high frequency kerr effect, electrostrictive effect, and thermal effect.[21–23]

2.1.1. Nuclear movement

The vibration or rotation of the nuclei (or ions) inside the medium molecule. This also contributes to the change in the refractive index of the medium. This contribution can be understood as the modulation effect on the optical frequency distortion of the molecular electron cloud. The response time of this process is about 10^{-12} s–10^{-14} s.[24]

2.1.2. High frequency Kerr effect

When the molecules are reoriented, the nonlinear refractive index of the material will be affected. When the laser acts on a fluid material composed of anisotropic molecules, the molecules will have different molecular polarizabilities and specular Kerr effects in different directions. The response time is about 10^{-11} s–10^{-12} s.[25–27]

2.1.3. Electrostrictive effect

Under the action of an optical frequency electric field, the molecules of matter are polarized. Along the direction of the light field, it is subjected to stress proportional to the intensity gradient. Thereby forming elastic mechanical motion. The density of the medium changes, resulting in a change in the refractive index of the material. The response time is in the range of 10^{-9} s–10^{-10} s.[28–30]

2.1.4. Thermal effect

When exposed to laser radiation, the medium will absorb part of the laser energy. The absorbed light energy is converted into heat energy through the non-radiative transition of particles in the medium. It causes a local temperature rise and a change in the density of the medium, which causes a change in the refractive index of the medium. Its response time is affected by many factors.[31–34]

2.2. Nonlinear absorption mechanisms

2.2.1. Saturable absorption and reverse saturable absorption

Saturable absorption (SA) means that the absorption coefficient of the medium decreases as the incident light intensity increases.[35,36] But when the light intensity increases to a certain extent, the electron absorbs the photon and transitions from the ground state to the excited state. At this time, the system is in a high energy state, that is, an unstable state. Then part of the electrons gradually returned to a low energy state. Eventually, the two processes of transition from ground state to excited state and transition from excited state to ground state form a dynamic equilibrium. The transition between bands is blocked. At this point, the material no longer absorbs photons. It can be considered that the material is "bleached", *i.e.*, photons can pass through the medium without loss. Reverse saturable absorption (RSA) refers to the phenomenon that the absorption coefficient of the medium also increases with the increase of the intensity of the emitted light under strong light.[37,38]

2.2.2. Two-photon absorption and multi-photon absorption

The two-photon absorption (TPA) process is shown in Fig. 2. Two photons are simultaneously absorbed by some medium. Crossed the intermediate state of the dotted line. From the initial state S_0 to the final state S_n, twice the photon energy is obtained. Generally, the two-photon absorption effect will increase as the light intensity increases. In addition, TPA has a high spatial selectivity.[39,40] There are two types of TPA: one is called direct transition, and its process is only photon transition. That is, electrons can directly absorb the photon transition from the ground state to the excited state. The another is called an indirect transition. The difference is that it also contains a phonon transition, which is caused by the inability of electrons to directly transition to an excited state. Therefore, when the energy of the photon is exactly the difference between the two energy poles, the atom will absorb two photons at the same time to complete the transition. Therefore the TPA process has good spatial selectivity and less damage to the sample.[41,42]

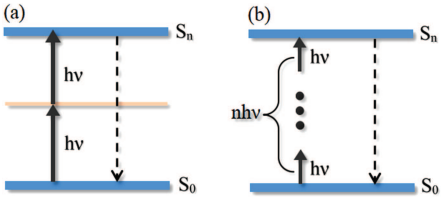


Fig. 2. (a) Schematic illustration of the two-photon absorption energy transfer process. (b) Schematic illustration of the multi-photon absorption energy transfer process.

The TPA needs to satisfy the condition that the band gap is between one photon energy and two photon energies. When the forbidden band width is larger, three-photon or multi-photon absorption (MPA) will occur. The MPA process is shown in Fig. 3. The MPA means that matter absorbs multiple photons at the same time, and can transit from the initial state to the final state only through the virtual state in the middle.[43] The MPA may be accompanied by multi-photon emission and multi-photon effects such as conductance, photoelectricity, fluorescence, dissociation, and photochemical reactions, which in turn contribute to the study of MPA processes.[44–46]

2.2.3. Free carrier absorption

Free carrier absorption (FCA), this mechanism mainly occurs in semiconductor nonlinear materials.[47,48] After the electrons in the valence band absorb incident photons and transition to the conduction band to generate carriers, these electrons (holes) are excited by the additionally absorbed photons to a higher state in the conduction band. This mechanism is similar to the mechanism of RSA, with the increase of light intensity, the nonlinear absorption increases.[49,50]

2.3. Nonlinear scattering

As light passes through any medium other than vacuum, part of the energy deviates from the predetermined direction of propagation, diffusing in space in any direction. This phenomenon is called light scattering. In NLO, there are two major types of nonlinear scattering (NLS) effects:[51,52] One is the higher-order scattering effects related to the higher-order nonlinear polarizability of the material. The other type is the stimulated scattering effect generated under high pump light intensity. The former is an important method to characterize the nonlinear polarizability tensor of materials. The latter has important applications in the fields of optical amplifiers, dynamic optical mirrors, and phase conjugate waves.[53]

3. Nonlinear optical properties of graphene and its compounds

3.1. Nonlinear optical properties studies of graphene

3.1.1. Graphene

Due to large specific surface area, high electron mobility, adjustable optical band gap, and easy surface modification, graphene has gradually been applied by scientists to the field of NLO research in recent years.[54–62] Marinko Jablan *et al.* investgated that graphene possesses a strong nonlinear optical response in the form of multiplasmon absorption, with exciting implications in classical and quantum nonlinear optics (in Fig. 3(a)). By increasing the intensity, there is an increase in the total damping rate and a decrease of the absorption cross section (in Fig. 3(b)).[58] Graphene obtained by different preparation methods or other treatments also has many NLO properties, such as RSA, SA, TPA, and FWM effect.[63–67] Therefore, graphene has become a new potential

material in the field of NLO. In recent years, a large number of studies have shown that graphene has NLO properties that are different from traditional materials. And its surface can be modified with different materials to exhibit different NLO properties.[68–70]

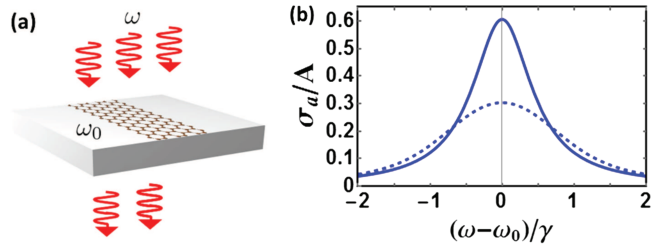


Fig. 3. (a) Transmission spectroscopy of a graphene nanoribbon. (b) Absorption cross section normalized to the surface area of the ribbon. The solid line stands for the low pump, and the dashed line for the high pump intensity. The saturation of absorption is caused by two plasmon absorption inside of the ribbon. Reproduced with permission from Ref. [59].

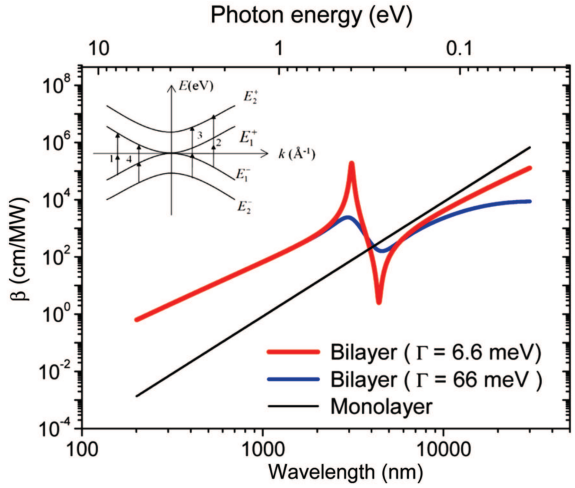


Fig. 4. The 2PA spectra of monolayer and bilayer graphene. Inset shows four possible transitions in bilayer graphene. When the incident photon energy $\hbar\omega > \gamma_1$, there are 4 possible inter band transitions: from lower price band (E_2^-) to conduction band (E_1^+ or E_2^+), from higher price band (E_1^-)) to conduction band (E_1^+ or E_2^+). where γ_1 is the hopping energy between two atom Reproduced with permission from Ref. [75].

Based on these excellent characteristics of graphene, its related research in the field of nonlinear optics has achieved many achievements. Hendry investigated the NLO properties of graphene flakes using FWM. The corresponding third-order optical susceptibility is found to be remarkably large and only weakly dependent on the wavelength in the near-infrared frequency range.[71] Marinko Jablan found that graphene possesses a strong nonlinear optical response in the form of multiplasmon absorption.[64,72,73] Cheng *et al.* studied that graphene dispersions exhibit enhancing NLO response. And its nonlinear absorption coefficient β is 2.89 cm/GW under 532-nm laser (6 ns, 2 Hz).[74] Yang *et al.* presented a quantum perturbation theory on TPA in monolayer and bilayer graphene which is Bernalstacked. As shown in Fig. 4, the theory shows that TPA is significantly greater in bilayer graphene than monolayer graphene in the visible and infrared spectrum (up to 3 μm) with a resonant 2PA coefficient of up to ∼ 0.2 cm/W located at half of the bandgap energy, $\gamma = 0.4$ eV.[75] Gullans *et al.* taked advantage of the electric field enhancement associated with the strong confinement of graphene plasmons and the large intrinsic nonlinearity of graphene, which it is possible to realize significant nonlinear optical interactions at the few photon level in graphene nanostructures.[76]

In recent years, graphene has repeatedly made important progress in *Q*-switched and mode-locked solid-state lasers.[77–79] Xu *et al.* successfully obtained 1.06 μm *Q*-switching and mode-locking operation with Nd:GdV04 crystal. The shortest *Q* pulse width is 105 ns, the maximum pulse energy is 3.2 μJ, and the output power can reach 2.3 W.[80] Demetriou *et al.* studied the nonlinear optical properties of multilayer graphene in the infrared region (1150, 1550, 1900, and 2400 nm). It is found that graphene has a significant nonlinear refraction effect in the infrared band.[81] Bao *et al.* found that graphene is used as a saturable absorber in erbium-doped fiber mode-locked lasers. A mode-locked laser with a center wavelength of 1565 nm, an average power of 2 mW, and a pulse of 756 fs was obtained.[82] Sun *et al.* used graphene to achieve a 460-fs mode-locked laser in a silver-doped laser.[83] Zhao *et al.* used graphene to obtain a mode-locked pulse of 580 ps in ytterbium-doped fiber.[84] Tan *et al.* used graphene bulk crystals for the first time to achieve mode locking. Finally, a 4-ps mode-locked pulse is obtained in the Nd:YAG laser.[85] Yu *et al.* found that graphene/$SrTiO_3$ has high response and fast response speed, which makes it have great potential in nonlinear optics.[86] Peng *et al.* Studied the tunable transmission properties of the proposed graphene ade structure in terahertz band, including the influence of Fermi level, asymmetry, structural parameters and operating frequency. The research results are helpful to better understand the tunability mechanism of graphene devices, and provide reference for the design of new high *Q* factor devices such as sensors, modulators, and filters in the future.[87] Li *et al.* have fabricated graphene bonded fiber devices. It is the first time that the nonlinear optical absorption of graphene is temperature-dependent through thermal relaxation process. The configuration is simple, cost-effective, and can be easily extended to other 2D materials (such as black phosphorus, transition metal disulfide, *etc.*).[88]

3.1.2. Graphene oxide

Graphene oxide is different from graphene in that its structural edges or defects contain a large number of oxygen-containing functional groups, so its properties are more active than graphene.[89,90] Graphene oxide obtains graphene after reduction, which leaves a large number of defects on the surface of the reduced graphene.[91] Therefore, the reduced graphene oxide not only has the hydrophilicity and lipophilicity of graphene oxide, but also has similar physical structures and chemical properties, these unique properties and structures

have also opened a whole new door for researchers to develop their applications in the field of nonlinear optics.[92]

Graphene oxide can show different nonlinear responses under different experimental conditions. Lim *et al*. investigated dispersed graphenes oxide (its schematic structure is shown in Fig. 5.) can exhibit broadband nonlinear optical absorption. For nanosecond visible and near-infrared pulses, a new benchmark for optical energy-limiting onset of 10 mJ/cm^2 for a linear transmittance of 70%.[75] In Fig. 6, Liu *et al*. found that as the input intensities increases from 2.1×10^9 W/cm^2 to 4.5, 10, and 34×10^9 W/cm^2, GO gradually changes from SA response to RSA.[93] Sukhdev Roy investigated that the RSA–SA transition occurs at higher concentration for higher values of I_0, as shown in Fig. 7.[94]

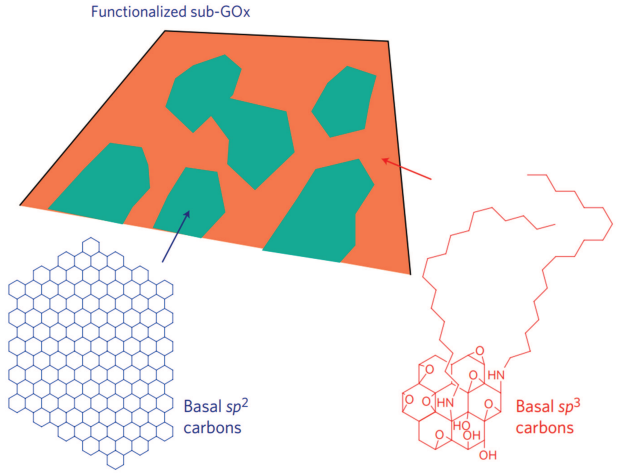


Fig. 5. Schematic structure of a functionalized sub-GO$_x$ sheet. The sheets contain functional groups composed of SP3 carbon atoms (orange) and nanographene regions (blue–green). Reproduced with permission from Ref. [73].

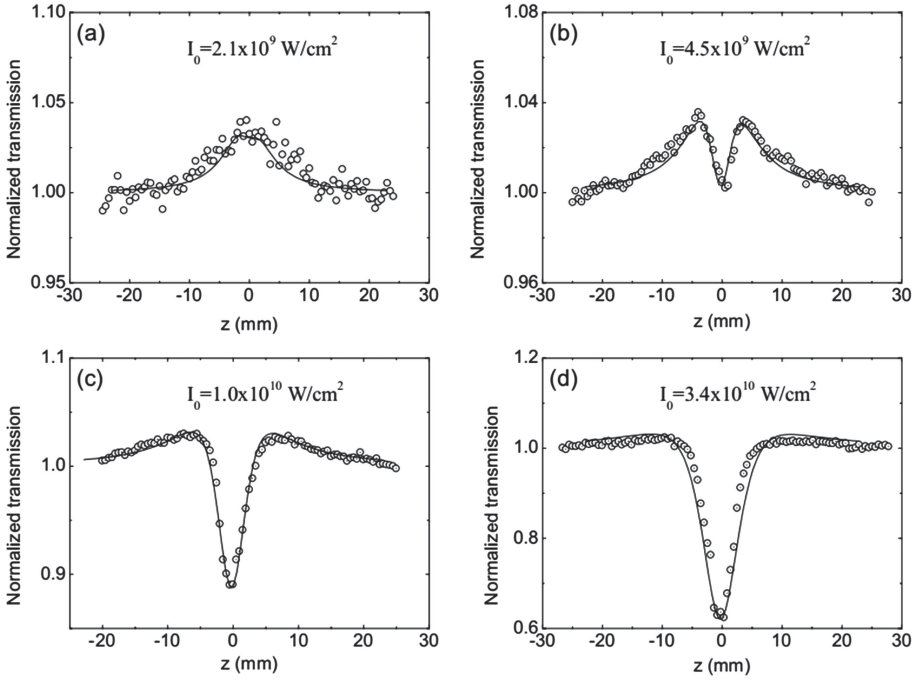


Fig. 6. Open aperture *Z*-scan curves of GO in DMF under different laser intensities, I_0 is the incident light intensity. Reproduced with permission from Ref. [93].

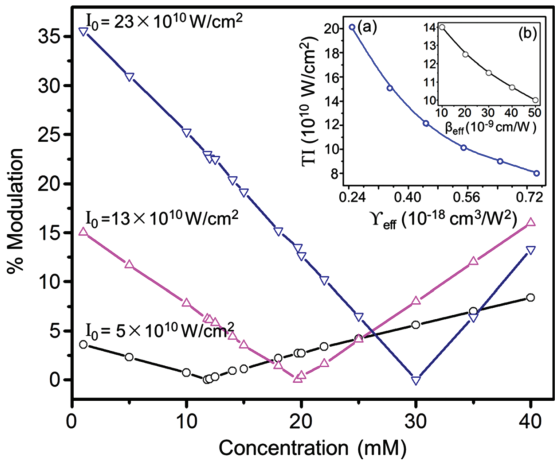


Fig. 7. Variation of percentage modulation with concentration. Inset shows the variation of SA to RSA transition intensity with (a) γ_{eff} and (b) β_{eff}. Reproduced with permission from Ref. [94].

Table 1. Nonlinear optical parameters of graphene and its composites.

Samples	Status	Laser parameters (wavelength λ, pulse duration τ, repetition rate ν)	Nonlinear optical parameters	Theoretical mechanism	Author
G	single sheets	$\lambda = 532$ nm $\tau = 3.5$ ns	$F_{th} = 0.01$ J/cm^2	NLA+NLS	Lim *et al.* 2011 (Ref. [73])
G	DMF dispersion	$\lambda = 532$ nm $\tau = 3.5$ ns $\nu = 2$ Hz	$\beta = 2.89$ cm/GW	NLA+NLS	Cheng *et al.* 2013 (Ref. [74])
GO	monolayer	$\lambda = 532$ nm $\tau = 800$ fs	$\beta = 1.37$ cm/GW	RSA+TPA+NLS	Krishna *et al.* 2012 (Ref. [48])
G–Au	solution	$\lambda = 532$ nm $\tau = 15$ ns $\nu = 1$ Hz	$\beta = 46$cm/GW $F_{th} = 0.4$ J/cm^2	RSA+NLS+NLS	Pradhan *et al.* 2015 (Ref. [96])
G–Au	nanorod	$\lambda = 1064$ nm $\tau = 30$ ps $\nu = 1$ Hz	$\beta = -3.39$ cm$\times 10^5$/GW	SA	Guo *et al.* 2017 (Ref. [97])
G–Ag	solution	$\lambda = 532$ nm $\lambda = 532$ nm	$\beta = 812$ cm/GW $\beta = 600$ cm/GW	RSA+TPA+NLS	Kalanoor *et al.* 2012 (Ref. [98])
GO–Pt	solution	$\lambda = 532$ nm $\tau = 4$ ns $\nu = 1$ Hz	$\beta = 1.1$ cm/GW $F_{th} = 0.32$ J/cm^2	RSA+TPA+NLS	Zheng *et al.* 2014 (Ref. [99])
GO–Pd	solution	$\lambda = 532$ nm $\tau = 4$ ns $\nu = 1$ Hz	$\beta = 1.0$ cm/GW $F_{th} = 0.4$ J/cm^2	RSA+TPA+NLS	Zheng *et al.* 2014 (Ref. [99])
GO–Au	solution	$\lambda = 532$ nm $\tau = 4$ ns $\nu = 1$ Hz	$\beta = 0.94$ cm/GW $F_{th} = 0.47$ J/cm^2	RSA+TPA+NLS	Zheng *et al.* 2014 (Ref. [99])
GO–Au	solution	$\lambda = 532$ nm	$n = 5.8$ cm^2/GW	RSA	Sadrolhosseini *et al.* 2014 (Ref. [100])
GO–Ag	solution	$\lambda = 532$ nm $\tau = 10$ ns	$\beta = 45.4$ cm/GW $n = 5.7 \times 10^{-3}$ cm^2/GW $X_3 = 16 \times 10^{-12}$ esu	NLR+TPA+ESA	Biswas *et al.* 2013 (Ref. [101])
G–ZnO	organic glasses	$\lambda = 532$ nm	$\beta = 1530$ cm/GW F $_{th} = 0.09$ J/cm^2	RSA+TPA+NLS	Ouyang *et al.* 2014 (Ref. [102])
G–CuO	solution	$\lambda = 1030$ nm $\tau = 340$ fs $\nu = 1000$ Hz	$\beta = 1.37$ cm/GW	TPA	Wu *et al.* 2018 (Ref. [103])
GO–Fe_3O_4	solution	$\lambda = 532$ nm $\tau = 35$ ps	$\beta = 26$ cm/GW $n = 2.83 \times 10^{-4}$ cm^2/GW $F_{th} = 2.33$ J/cm^2	TPA+RSA	Zhang *et al.* 2011 (Ref. [104])
GO–SiO_2	solution	$\lambda = 532$ nm	$n = 8.5$ cm^2/GW	NLR	Hamid Darabi *et al.* 2019 (Ref. [105])
G–CdS	organic glasses	$\lambda = 532$ nm $\tau = 6$ ns $\nu = 1$ Hz	$\beta = 797$ cm/GW	TPA+RSA+FCA	Ouyang *et al.* 2013 (Ref. [106])
GNS-CdS	solution	$\lambda = 532$ nm $\lambda = 1064$ nm	$F_{th} = 0.88$ J/cm^2 $F_{th} = 6.4$ J/cm^2	NLS+FCA	Mian Feng *et al.* 2010 (Ref. [107])
G–MoS_2	organic glasses	$\lambda = 532$ nm $\tau = 6$ ns $\nu = 1$ Hz	$\beta = 2110$ cm/GW	RSA+TPA	Ouyang *et al.* 2013 (Ref. [108])
G–Ag_2S	organic glasses	$\lambda = 532$ nm $\tau = 6$ ns $\nu = 1$ Hz	$\beta = 2560$ cm/GW	RSA+TPA	Ouyang *et al.* 2013 (Ref. [109])
GO–ZnS	solution	$\lambda = 1030$ nm $\tau = 340$ fs $\nu = 1000$ Hz	$\beta = 554.9$ cm/GW	RSA+3PA	Li *et al.* 2020 (Ref. [110])
rGO–CdSe	solution	$\lambda = 532$ nm $\tau = 30$ ps $\nu = 10$ Hz	$\beta = 224.42$ cm/GW $n = 4.9 \times 10^{-10}$ cm^2/GW $X_3 = 164.49 \times 10^{-12}$ esu	RSA+NLR	Li *et al.* 2019 (Ref. [111])
GO–PbS	organic glasses	$\lambda = 532$ nm $\tau = 4$ ns	$\beta = 79$ cm/GW $F_{th} = 2.3$ J/cm^2	RSA+TPA	Zhao *et al.* 2013 (Ref. [112])
GO–NH_2-Pani	solution	$\lambda = 532$ nm $\tau = 5$ ns	$\beta = 8.5$ cm/GW $F_{th} = 0.8$ J/cm^2	RSA+TPA+NLS	Remyamol *et al.* 2013 (Ref. [113])
G-6THIOP	solution	$\lambda = 532$ nm $\tau = 5$ ns $\nu = 10$ Hz	$F_{th} = 0.15$ J/cm^2	RSA+TPA	Zhang *et al.* 2009 (Ref. [115])
G–Cu porphyrin	solution	$\lambda = 532$ nm	$\beta = 4720$ cm/GW	TPA	Bala Murali Krishna *et al.* 2011 (Ref. [116])
G–Zn porphyrin	solution	$\lambda = 532$ nm	$\beta = 3570$ cm/GW	TPA	
G–DNA	solution	$\lambda = 1064$ nm $\tau = 125$ fs $\nu = 1000$ Hz	$\beta = 2.26$ cm/GW	RSA+TPA+NLS	Husaini *et al.* 2014 (Ref. [118])
GNR–ER	solution	$\lambda = 532$ nm	$n = 2.6$ cm^2/GW $F_{th} = 2.4$ J/cm^2	NLR	Al-Asadi *et al.* 2019 (Ref. [119])

3.2. Nonlinear optical properties studies of G-MNPs

In summary, most of the reported optical limiting properties of graphene and graphene oxide are mainly due to TPA and NLS.[95] However, due to the zero band gap and weak light absorption properties of graphene, general pure graphene materials are not considered as ideal OL materials. Therefore, the researchers have attempted to modify other nanoparticles on the surface of graphene, and the results showed that their

light absorption properties can be effectively adjusted, thereby improving their NLO properties. As shown in Table 1, Prabin Praghan *et al*. demonstrated that d-orbitals of Au nanoparticles exhibit little or no rehybridization with graphene and result in an enhanced optical limiting behavior at a low fluence of 0.4 J/cm^2.[96] All samples used in this study exhibited OL performance due to significant NLS at higher intensities (Fig. 8(a)). As shown in Fig. 8(b), the exf-graphene and Au NPs do not show significant OL threshold whereas in the case of Au-graphene, the transmittance decreases sharply indicating strong OL effect at lower thresholds, which is ideal for practical applications. Kalanoor *et al*. found that drastic changes in the *Z*-scan profiles are obtained in AgNP/fG at 1064 nm as the profile flips from the behavior of strong saturable absorption (SA) to reverse saturable absorption (RSA) on increasing the incident intensity.[98] It is investigated that the extracted value of third order nonlinear susceptibility (χ_3), at a peak intensity of $I_0 = 0.2$ GW/cm^2, for GO–Ag has been found out to be 2.8 times larger than that of GO. Zheng *et al*. synthesized a series of graphene oxide (GO)/noble metal (Au, Pt, and Pd) nanoparticle (NP) composites via a one-step hydrothermal reaction. The corresponding nonlinear optical (NLO) and optical limiting (OL) properties were investigated using an open-aperture *Z*-scan technique 10 with nanosecond pulses at 532 nm. Results show that the NLO and OL properties were significantly enhanced after the inclusion of metal NPs onto the GO surface because of nonlinear scattering (NLS) effects.[99]

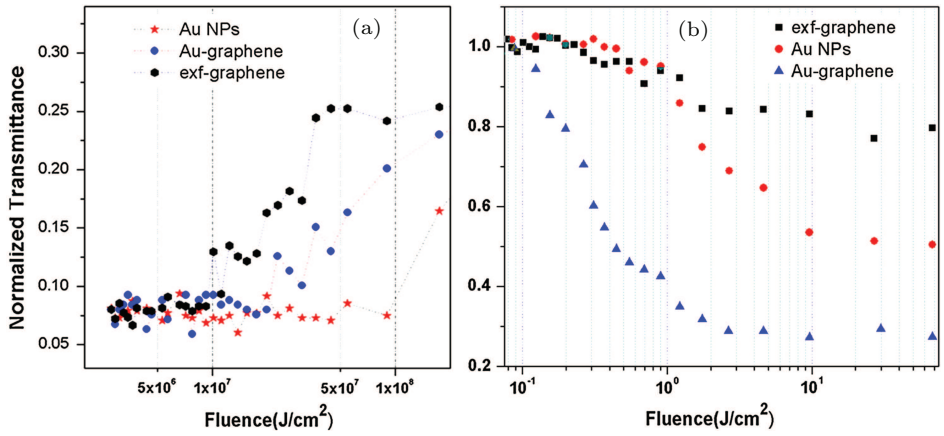


Fig. 8. (a) The NLS signal of Au NPs, Au–graphene, and exf-graphene recorded by a calibrated photodetector. (b) The optical limiting response of Au NPs, exf-graphene, and Au–graphene dispersions. Reproduced with permission from Ref. [96].

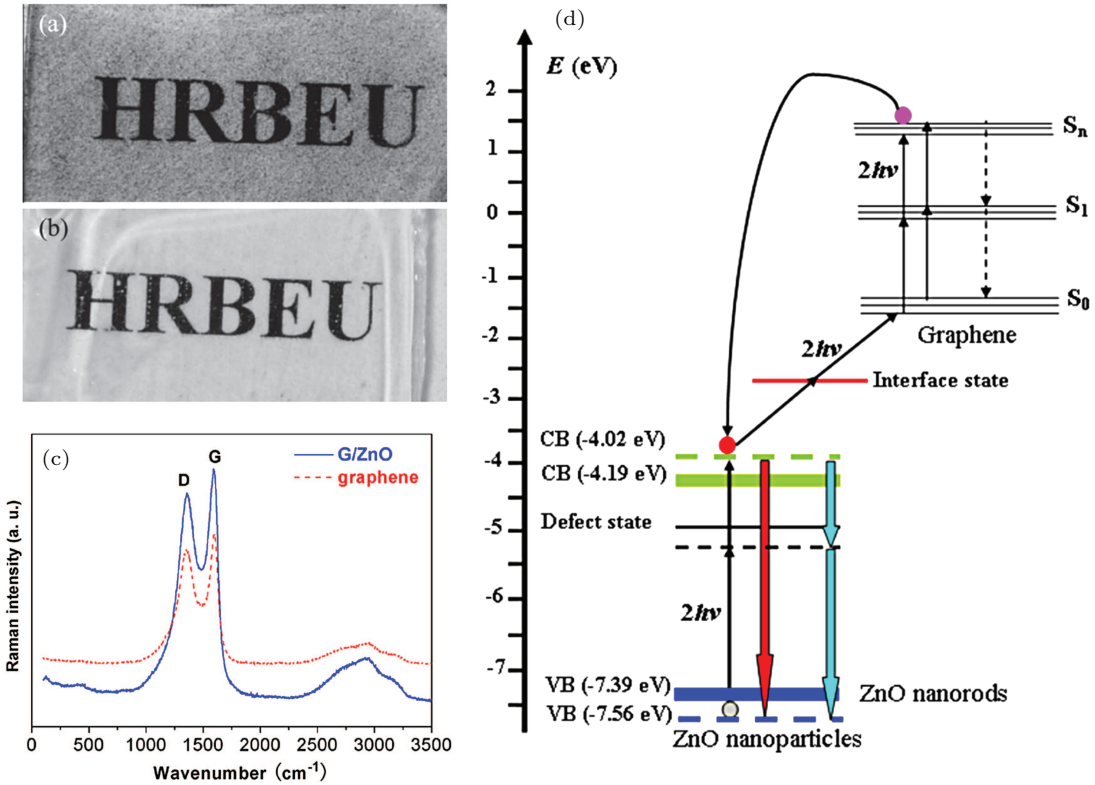


Fig. 9. (a) Photograph of G–ZnO/PMMA organic glasses. (b) Photograph of ZnO/PMMA organic glasses. (c) Raman spectra of G/ZnO composites and graphene. (d) Energy level diagram of G/ZnO composites, reproduced with permission from Ref. [102].

3.3. Nonlinear optical properties studies of G-MONPs

Ouyang *et al*. synthesized graphene/ZnO(G/ZnO) composite material for the first time by wet chemical method.[102] The results showed that the NLO properties of the G/ZnO composite is significantly enhanced. Figures 9(a) and 9(b) show photographs of G–ZnO/PMMA and ZnO/PMMA organic glasses, respectively. The Raman spectra of G/ZnO composites and graphene are shown in Fig. 9(c). The D and G bands of the G/ZnO composite have blue shift and red shift, respectively. The results showed that there is an interaction between graphene and ZnO nanoparticles. This interaction is believed to promote charge transfer between graphene and ZnO nanoparticles.[72,73] Wu *et al*. measured the NLA coefficient of G–CuO at 1030-nm wavelength laser (340 ps, 1000 Hz) $\beta = 1.37$ cm/GW, which was enhanced compared to pure graphene.[103] Zhang studied that GO–Fe_3O_4 exhibits enhanced NLO and OL properties in comparison with the pristine GO in the nanosecond regime. As shown in Fig. 10(a), the effective TPA coefficient β_{eff} is nearly a constant of 7 cm/GW at different input intensities for GO, indicating the dominant TPA mechanism. Figure 10(b) shows the open-aperture and closed-aperture Z-scan results of GO–Fe_3O_4, which indicated stronger NLA/NLS exists.[104]

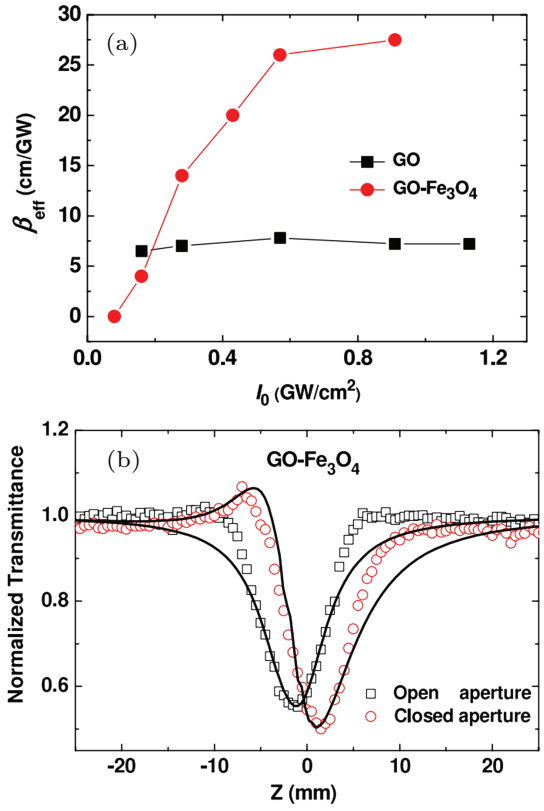


Fig. 10. (a) The values of the effective TPA coefficient β_{eff} as a function of on-axis peak intensity for GO and GO–Fe_3O_4 with the same concentration of 0.375 mg/ml in the case of nanosecond pulses. (b) Open-aperture and closed-aperture Z-scan curves of GO–Fe_3O_4 with nanosecond pulses, reproduced with permission from Ref. [104].

3.4. Nonlinear optical properties studies of G–MSNPs

The researchers have found that modifying the sulfide nanoparticles on the graphene surface to adjust the band gap is also an effective way to improve nonlinearity. The G/CdS/PMMA organic glass exhibits enhanced NLO properties compared to G/PMMA and CdS/PMMA organic glass is reported.[106,107] Figure 11 presents its Z-scan curve, the results show the NLO properties of the G/CdS/PMMA organic glass can be controlled by adjusting the addition amount of G/CdS nanocomposite in PMMA. Another literature reported that the G/MoS_2 organic glasses (the NLA coefficient b, was up to 2110 cm/GW) exhibited enhanced RSA properties compared to G ($\beta = 242$ cm/GW) and MoS_2 ($\beta = 365$ cm/GW) organic glasses.[108] Similarly, it is investigated that the G/Ag_2S/PMMA organic glass with an appropriate amount of G/Ag_2S exhibited enhanced reverse saturable absorption (RSA) properties compared to G/PMMA and Ag_2S/PMMA organic glasses, which was attributed to the notable synergistic effects between graphene and Ag_2S.[108] Li *et al*. studied that decorating ZnS nanoparticles on the surface of graphene can effectively enhance its OL performance.[109] Min Zhao studied that the rGO–PbS nanohybrid exhibited superior OL properties to either GO or PbS QDs upon both 532-nm and 1064-nm excitations in the nanosecond laser pulse regime, which is attributed to the synergetic effects stemming from charge transfer between the two components.[110] As shown in Fig. 12(a), the rGO–PbS presents RSA properties. Figure 12(b) indicated that the mechanism of the OL properties of rGO–PbS system is expected to be a result of combination of FCA and NLS. Feng research group found that CdS QDs with an average diameter of 3 nm are uniformly dispersed over the surface of graphene, and the resulting quantum dots-graphene composite exhibits excellent OL properties, mainly contributed by NLS and NLA, upon both 532-nm and 1064-nm excitations, in the nanosecond laser pulse regime. Its OL threshold determined as ~ 0.88 and > 6.4 J/cm^2 at 532 nm and 1064 nm, respectively, and its limiting performance is much pronounced at 532 nm as compared to that in the near infrared region (1064 nm).[106]

3.5. Nonlinear optical properties studies of G–OM

Recent studies have shown that loading certain organic molecules on the surface of graphene can effectively adjust its light absorption properties, thereby improving its nonlinear optical properties. Remyamol *et al*. successfully synthesized and found that rGO covalently decorated with polyaniline (GO–NH_2-Pani) showed improved NLO properties compared to the GO precursor and the pristine polyaniline.

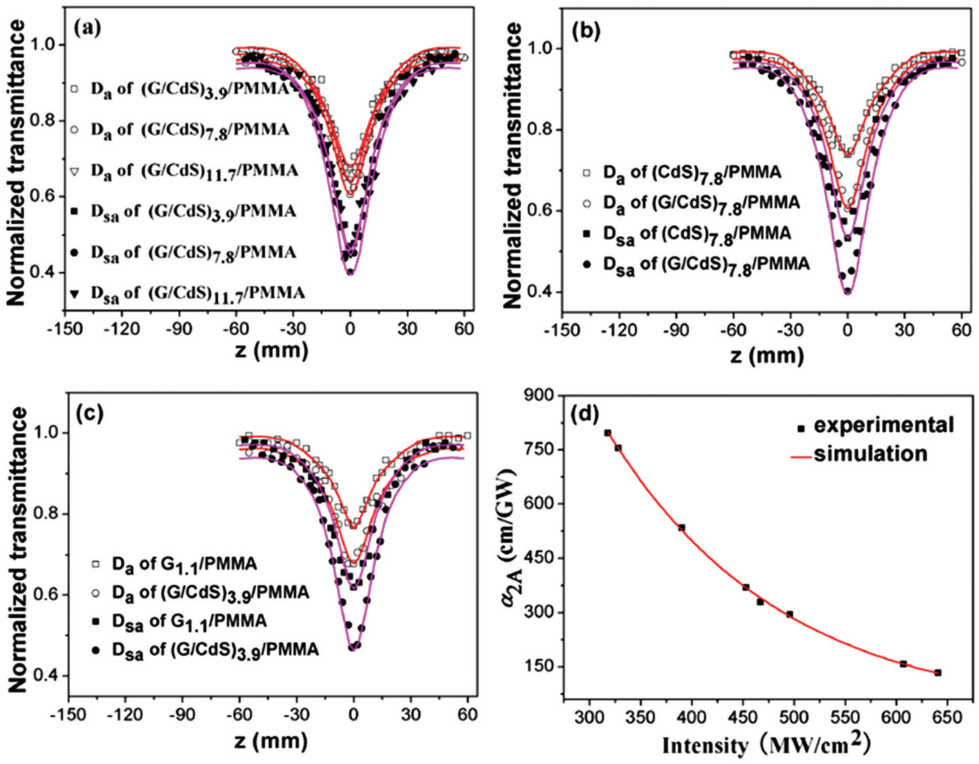


Fig. 11. NLA and NLS curves of (a) G/CdS/PMMA organic glass with different amounts of G/CdS; (b) $(G/CdS)_{7.8}$/PMMA and (CdS)7.8/PMMA organic glass; and (c) $(G/CdS)_{3.9}$/PMMA and $G_{1.1}$/PMMA organic glass. (d) NLA coefficient α_{2A} of $(G/CdS)_{7.8}$/PMMA organic glass as a function of input intensity, reproduced with permission from Ref. [106].

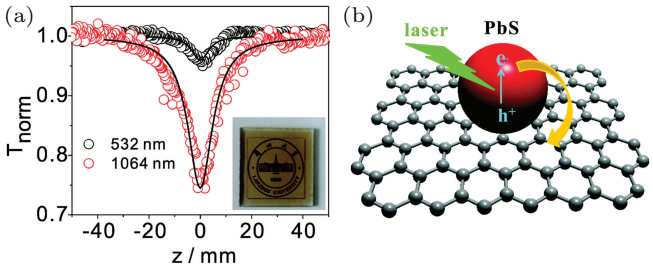


Fig. 12. (a) Open aperture *Z*-scan data and theoretically fitted curves for a neat film of rGO–PbS in poly irradiated by 4-ns pulses at 532 nm and 1064 nm. (b) Schematic illustration of charge and energy transfer between PbS QDs and rGO, reproduced with permission from Ref. [112].

Figure 13 shows the OL curves of GO, Pani, and GO–NH_2–Pani, respectively. The improvement in the OL performance of the hybrid is attributed to a combination of outstanding properties of GO and polyaniline, like NLS, TPA, and RSA.[113] Zhang *et al*. firstly synthesized G–C_{60} hybrid mterials and found that its enhanced NLO performance better than its parent species C_{60} and graphene may be attributed at least partially to the photoinduced-electron transfer mechanism between the graphene sheet and C_{60}.[114] Zhang *et al*. found that the NLO and OL properties of an oligothiophene (6THIOP) covalently functionalized graphene hybrid material (graphene-6THIOP) were enhanced than that of graphene or 6THIOP.[115] The NLO properties of covalently linked graphene–metal porphyrin composite materials is investigated in Ref. [116].

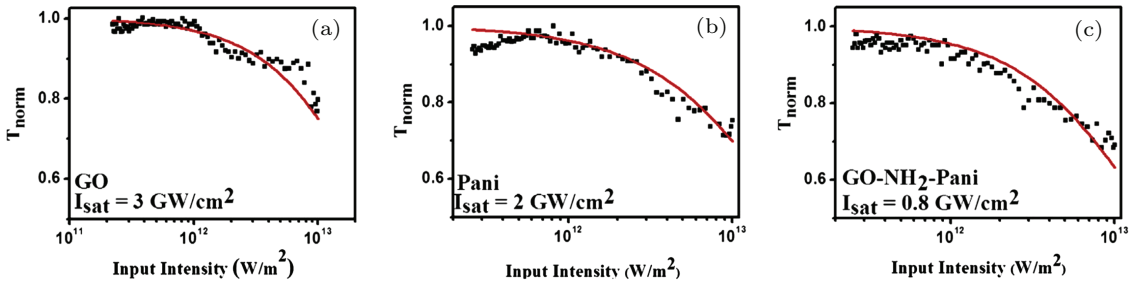


Fig. 13. Optical limiting curves of (a) GO, (b) Pani, and (c) GO-NH_2-Pani. Reproduced with permission from Ref. [113].

Figure 14 shows the result of *Z*-scan test in nanosecond regime. Table 2 shows the specific data of *Z*-scan curve fitting. It can be seen the NLO coefficients of graphene–copper porphyrin and graphene–zinc porphyrin is 4720 cm/GW and 3570 cm/GW, which is 5.24 times and 3.97 times than that of pure graphene. Wang *et al*. studied that graphene oxide axially-coordinated

tetraphenylporphyrin (GO–TPP) nanohybrids exhibited enhanced NLO properties and OL performance, ascribed to a combination of NLS and/or TPA with RSA, and the photoinduced electron or energy transfer from the electron–donor porphyrin moiety to the acceptor graphene.[117] Husaini *et al.* found that G–DNA composite film when irradiated with nanosecond pulses indicates a damage threshold > 50 J/cm^2.[118] Al-Asadi *et al.* successfully synthesized the graphene nanosheets–epoxy resin (GNR-ER) composite material and measured its nonlinear refractive index as -2.6 cm^2/GW.[119]

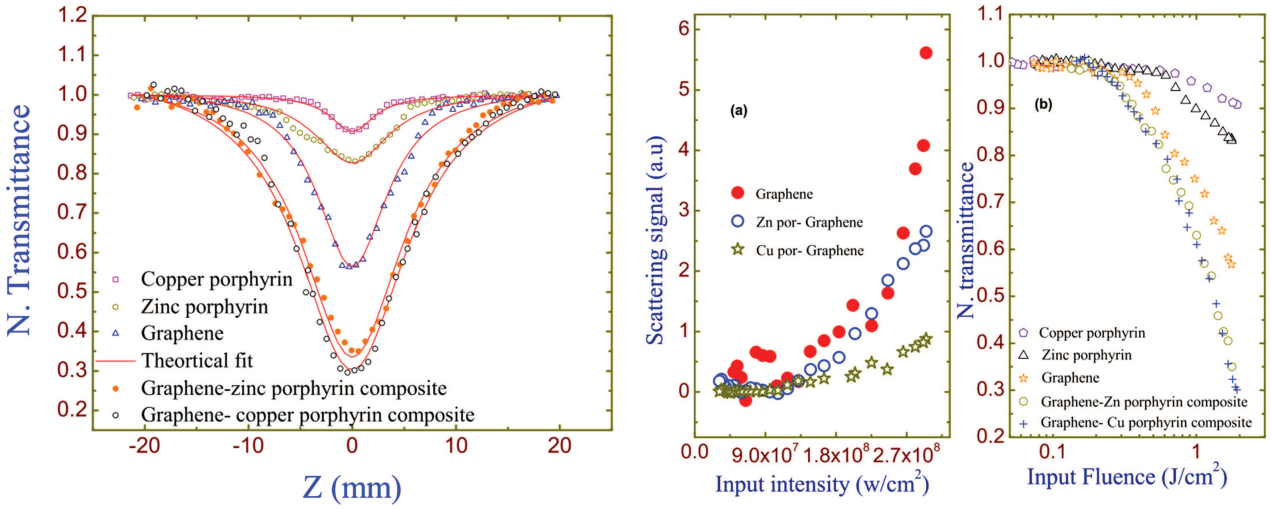


Fig. 14. (a) Scattering signal with input intensity of graphene and graphene–porphyrin composites. (b) Optical limiting curves. (c) Open aperture *Z*-scan curves of of copper porphyrin, zinc porphyrin, graphene, graphene–zinc porphyrin, and graphene–copper porphyrin composites in DMF at 532 nm in nanosecond, reproduced with permission from Ref. [116].

Table 2. Excited state and ground state parameters δ_0, $\delta_{\text{eff}}^{\text{ex}}$, β, τ_{sl}, and τ_{sn} for copper porphyrin, zinc porphyrin, pure graphene, and graphene–porphyrin composites at 532 nm in nanosecond time scales.[116]

Samples	δ_0 (10^{-19} cm^2)	$\delta_{\text{eff}}^{\text{ex}}$ (10^{-19} cm^2)	β (cm/GW)	FOM ($\delta_{\text{eff}}^{\text{ex}}/\delta_0$)	τ_{sl} (ns)	τ_{sn} (ps)
Copper porphyrin	4	79	132	19.75	0.9	6
Zinc porphyrin	4.4	113	366	25.68	0.78	5
Pure graphene	5.3	30.1	900	5.68	0.009	0.009
Graphene–copper porphyrin	8.3	380	4720	45.78	0.5	7
Graphene–zinc porphyrin	4.9	214	3570	43.67	0.68	9

4. Conclusions

As a new type of nonlinear optical material, graphene can exhibit the characteristics of RSA, SA, and TPA under different experimental conditions.[120,121] This paper comprehensively describes the nonlinear response of graphene, graphene oxide, and their composite materials. Modulation of graphene band gap by composite of other species on the surface of graphene has become an important means to enhance its NLO response. The enhancement mechanism is mainly divided into the following three parts:[122,123] (i) Charge transfer mechanism between graphene and nanoparticles; (ii) A large number of defects caused by the small size effect of nanoparticles will become the scattering center, resulting in enhanced NLS; (iii) Bubbles caused by thermal effects cause nonlinear refraction enhancement.

In summary, the nonlinear enhancement caused by graphene compounding makes it have greater application potential in the field of OL materials (in Fig. 15). However, its enhancement mechanism needs to be verified by specific experimental theory. The practical application of graphene composite materials in the field of nonlinear optics still faces many challenges.

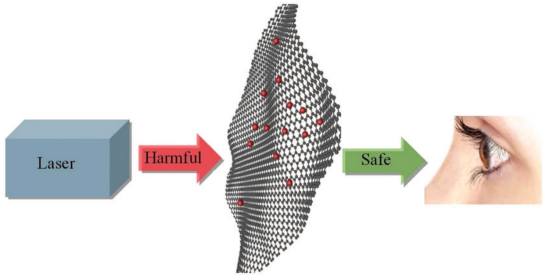


Fig. 15. Application of graphene and its composite materials in the field of optical limiting.

References

[1] Boyd R W and Masters B R 2009 *J. Biomed. Opt.* **14** 029902
[2] Harris S E and Hau L V 1999 *Phys. Rev. Lett.* **82** 4611
[3] Horikis T P and Elgin J N 2004 *Phys. Rev. E* **69** 016603
[4] Brabec T and Krausz F 2000 *Rev. Mod. Phys.* **72** 545
[5] Goulielmakis E, Schultze M, Hofstetter M, Yakovlev V S, Gagnon J, Uiberacker M, Aquitaal A L, Gullikson E M, Attwood D T and Kienberger R 2008 *Science* **320** 1614

[6] Dudley J M, Finot C, Richardson D J and Millot G 2007 *Nat. Phys.* **3** 597
[7] Agranovich V M, Basko D M and Rocca G C L 2012 *Phys. Rev. B* **86** 165204
[8] Roberts R L, Schwich T, Corkery T C, Cifuentes M P, Green K A, Farmer J D, Low P J, Marder T B, Samoc M and Humphrey M G 2010 *Adv. Mater.* **21** 2318
[9] Wu J Y, Yang Y Y, Qu Y, Jia L N, Zhang Y N, Xu X Y and Chu S T 2020 *Small* **16** 1906563
[10] Litchinitser N M 2018 *Adv. Phys. X* **3** 1367626
[11] Brus L 1991 *Appl. Phys. A* **53** 465
[12] Tutt L W and Boggess T F 1993 *Prog. Quantum. Electron* **17** 299
[13] Sheik B M, Said A A, Wei T H, Hagan D and Van-Stryland E W 1990 *IEEE J. Quantum Electron.* **26** 760
[14] Long H, Yang G, Chen A, Li Y and Lu P 2009 *Opt. Commun.* **282** 1815
[15] Feng Z S, Li X M, Jing X Y, Lan Z H and Ning C D 2015 *Applied Mechanics & Materials* **713** 343
[16] Tsigaridas G, Fakis M, Polyzos I, Persephonis P and Giannetas V 2005 *J. Phys. Conf.* **10** 242
[17] Zhang H, Virally S, Bao Q, Ping L K, Massar S, Godbout N and Kockaert P 2012 *Opt. Lett.* **37** 1856
[18] Yan X Q, Liu Z B, Zhang X L, Zhou W Y and Tian J G 2009 *Opt. Express* **17** 6397
[19] Venkatram N, Rao D N and Akundi M A 2005 *Opt. Express* **13** 867
[20] Venkatram N, Kumar R S S and Rao D N 2006 *J. Appl. Phys.* **100** 13226
[21] Monot P, Doumy G, Dobosz S, Perdrix M and Geindre J P 2004 *Opt. Lett.* **29** 893
[22] Lobanov V E, Kalinovich A A, Sukhorukov A P, Bennet F and Neshev D 2009 *Laser Phys.* **19** 1112
[23] Shimamoto D, Sakurai T, Itoh M, Kim Y A, Hayashi T, Endo M and Terrones M 2008 *Appl. Phys. Lett.* **92** 081902
[24] Hao X F, Hao D S and Sun F Z 2011 *Nuclear Fusion and Plasma Physics* **31** 315
[25] Levinson O and Horowitz M 2003 *J. Lightwave Technol.* **21** 1179
[26] Freysz and Eric 2010 *Nat. Photon.* **4** 131
[27] Hoffmann M C, Hwang H Y, Brandt N C, Yeh K L and Nelson K A 2009 *Mrs. Proceedings* **1230** 08
[28] Guillot F M and Balizer E 2010 *J, Appl. Polym. Sci.* **89** 399
[29] Hall A, Allahverdi M, Akdogan E K and Safari A 2005 *J. Electroceram* **15** 143
[30] Tashiro S, Ishii K and Nagata K 2003 *Jpn. J. Appl. Phys.* **42** 6068
[31] Liu F, Li Q, Zhang Z, Qiu M and Su Y 2008 *IEEE J. Selec. Top. Quantum Electron.* **14** 706
[32] Xu L J and Huang J P 2020 *Chin. Phys. Lett.* **37** 080502
[33] Liu Z B, Shi S, Yan X Q, Zhou W Y and Tian J G 2011 *Opt. Lett.* **36** 2086
[34] Shapiro A and Kanak K M 2002 *J. Atmos. Sci.* **59** 2253
[35] Bao Q, Zhang H, Ni Z, Yu W, Polavarapu L, Shen Z, Xu Q H, Tang D and Loh K P 2011 *Nano. Res.* **4** 297
[36] Xing G, Guo H, Zhang X, Sum T C and Cheng H A H 2010 *Opt. Express* **18** 4564
[37] Mclean D G, Sutherland R L and Brant M C 1993 *Opt. Lett.* **18** 858
[38] Raghunathan V, Shori R, Stafsudd O M and Jalali B 2006 *Phys. Stat. Sol. (a)* **203** 38
[39] Pawlicki M, Hazel A C, Denning R G and Anderson H L 2008 *Angew. Chem. Inte. Edit.* **48** 18
[40] Cheng W D, Wu D S, Li X D, Lan Y Z, Zhang H, Chen D G, Gong Y J, Zhang Y C, Li F F and Shen J 2004 *Phys. Rev. B* **70** 2806
[41] Liu Y and Tsang H K 2006 *Opt. Lett.* **31** 1714
[42] Wang G Z, Bennett D, Zhang C F, Coileain C O, Liang M Y, McEvoy N, Wang J J, Wang K P, Nicolosi V and Blau W J 2020 *Adv. Opt. Mater.* **8** 1902021
[43] Husko C A, Clark A S, Collins M J, Rossi A D, Combrié S, Lehoucq G, Rey I H, Krauss T F, Xiong C and Eggleton B J 2013 *Sci. Rep-UK* **3** 3087
[44] Wang T, Venkatram N, Gosciniak J, Cui Y J, Qian G D, Ji W and Tan D T H 2012 *Opt. Express* **21** 32192
[45] Ganeev R A 2005 *J. Opt. A-Pure. Appl. Opt.* **7** 717
[46] Padilha L A, Webster S, Przhonska O V, Hu H H, Peceli D, Rosch J L, Bondar M V, Gerasov A O, Kovtun Y P, Shandura M P, Kachkovski A D, Hangan D J and Van Stryland E W 2009 *J. Mater. Chem.* **19** 7503
[47] Kioupakis E, Rinke P, Schleife A, Bechstedt F and Van de Walle C G 2010 *Phys. Rev. B* **81** 241201
[48] Zhang C and Cao J C 2004 *Phys. Rev. B* **70** 193311
[49] Yan M, Rickey E G and Zhu Y F 2001 *Opt. Lett.* **26** 548
[50] He J, Ji W, Ma G H, Tang S H, Elim H I and Sun W X 2004 *J. Appl. Phys.* **95** 6381
[51] Jiang Z L, Feng Z W, Liu Q Y, Jiang Y M and Liang H 2001 *Chin. J. Inorg. Chem.* **17** 355
[52] Roke S and Gonella G 2012 *Ann. Rev. Phys. Chem.* **63** 353
[53] Webster S, Fu J, Padilha L A, Przhonska O V, Hagan D J, Van Stryland E W, Bondar M V, Slominsky Y L and Kachkovski 2008 *Chem. Phys.* **348** 143
[54] Geim A K 2009 *Science* **324** 1530
[55] Bonaccorso F, Sun Z, Hasan T and Ferrari A C 2010 *Nat. Photon.* **4** 611
[56] Castro Neto A H, Guinea F, Peres N M R, Novoselov K S and Geim A K 2009 *Rev. Mod. Phys.* **81** 109
[57] Li X Y, Lin H, Zhao Y J and Jia B H 2020 *Chin. Phys. Lett.* **37** 106801
[58] Wang Y R, Tokman M and Belyanin A 2016 *Phys. Rev. B* **94** 195442
[59] Jablan M and Chang D E 2015 *Phys. Rev. Lett.* **114** 236801
[60] Chen X Y, Tian Z, Li Q, Li S X, Zhang X Q, Ouyang C M, Gu J Q, Han J G and Zhang W L 2020 *Chin. Phys. B* **29** 077803
[61] Son Y W, Cohen M L and Louie S G 2006 *Nature* **444** 347
[62] Son Y W, Cohen M L and Louie S G 2006 *Phys. Rev. Lett.* **97** 216803
[63] Zhang H, Stéphane V, Bao Q L, Ping L K, Massar S, Godbout N and Kockaert P 2012 *Opt. Lett.* **37** 1856
[64] Mikhailov S A and Ziegler K 2008 *J. Phys.: Condens. Matter* **20** 384204
[65] Sensale-Rodriguez B, Yan R, Kelly M M, Fang T, Hwang W S, Jena D, Liu L and Xing H G 2012 *Nat. Commun.* **3** 780
[66] Mikhailov S A 2009 *Microelectron. J.* **40** 712
[67] Vakil A and Engheta N 2012 *Phys. Rev. B* **85** 075434
[68] Park C H, Yang L, Son Y W, Cohen M L and Louie S G 2008 *Phys. Rev. Lett.* **101** 126804
[69] Martinez A and Sun Z 2013 *Nat. Photon.* **7** 842
[70] Xu J L, Li X L, Wu Y Z, Hao X P, He J H and Yang K J 2011 *Opt. Lett.* **36** 1948
[71] Maeng I, Lim S, Chae S J, Lee Y H, Choi H and Son J H 2012 *Nano Lett.* **12** 551
[72] Liaros N, Bourlinos A B, Zboril R and Couris S 2013 *Opt. Express* **21** 21027
[73] Lim G K, Chen Z L, Clark J, Goh R G S, Ng W H, Tan H W, Friend R H, Ho P K H and Chua L L 2011 *Nat. Photon.* **5** 554
[74] Cheng X, Dong N N, Li B, Zhang X Y, Zhang S F, Jiao J, Blau W J, Zhang L and Wang J 2013 *Opt. Express* **21** 16486
[75] Yang H Z, Feng X B, Wang Q, Huang H Chen W, Wee A T S and Ji W 2011 *Nano Lett.* **11** 2622
[76] Gullans M, Chang D E, Koppens F H L, Garcia de Abajo F J and Lukin M D 2013 *Phys. Rev. Lett.* **111** 247401
[77] Popa D, Sun Z, Hasan T, Torrisi F, Wang F and Ferrari A C 2011 *Appl. Phys. Lett.* **98** 073106
[78] Cao W J, Wang H Y, Luo Z C and Xu W C 2011 *Laser Phys. Lett.* **9** 54
[79] Popa D, Sun Z, Hasan T, Torrisi F, Wang F and Ferrari A C 2010 *Appl. Phys. Lett.* **97** 203106
[80] Xu J L, Li X L, He J L, Hao X P Yang Y, Wu J L, Liu S D and Zhang B T 2012 *Opt. Lett.* **37** 2652
[81] Demetriou G, Bookey H T, Biancalana F, Abraham E, Wang Y, Ji W and Kar A K 2016 *Opt. Express* **24** 13033
[82] Bao Q L, Zhang H, Wang Y, Ni A H, Shen Z X, Loh K P and Tang D Y 2009 *Adv. Funct. Mater.* **19** 3077
[83] Sun Z P, Hasan T, Torrisi F, Popa D Privitera G, Wang F Q, Bonaccorso F, Basko D M and Ferrari A 2010 *Acs Nano* **4** 803
[84] Zhao L M, Tang D Y, Zhang H, Wu X, Bao Q L and Loh K P 2010 *Opt. Lett.* **35** 3622
[85] Tan W D, Su C Y, Knize R J, Xie G Q, Li L J and Tang D Y 2010 *Appl. Phys. Lett.* **96** 031106
[86] Yue H, Hu A Q, Liu Q L, Tian H J, Hu C R, Ren X S, Chen N Y, Ge C, Jin K J and Guo X 2021 *Chin. Phys. B* **30** 038502
[87] Peng J, He X Y, Shi C Y, Leng J, Lin T T, Liu F, Zhang H and Shi W Z 2020 *Physica E* **124** 114309
[88] Li C, Chen J H, Wang W S, Wang T X, Yan S C, Li D R, Xu F, Mou C B and Lu Y Q 2017 *Adv. Opt. Mater.* **5** 1700630

[89] Tu Y S, Zhao L, Sun J J, Wu Y Y, Zhou X J, Chen L, Lei X L, Fang H P and Shi G S 2020 *Chin. Phys. Lett.* **37** 066803

[90] Morales-Narvaez E and Merkoci A 2012 *Adv. Mater.* **24** 3298

[91] Acik M, Lee G, Mattevi C, Chhowalla M, Cho K and Chabal Y J 2010 *Nat. Mater.* **9** 840

[92] Shi H F, Wang C, Sun Z P, Zhou Y L, Jin K J, Redfern S A T and Yang G Z 2014 *Opt. Express* **22** 19375

[93] Liu Z B, Wang Y, Zhang X L, Xu Y F, Chen Y S and Tian J G 2009 *Appl. Phys. Lett.* **94** 73

[94] Roy S and Yadav C 2013 *Appl. Phys. Lett.* **103** 241113

[95] Bala Murali Krishna M, Venkatramaiah N, Venkatesan R and Narayana Rao D 2012 *J. Mater. Chem.* **22** 3059

[96] Pradhan P, Podila R, Molli M, Kaniyoor A, Sai Muthukumar V, Siva Sankara Sai S, Ramaprabhu S and Rao A M 2015 *Opt. Mater.* **39** 182

[97] Guo J, Ning T Y, Han Y S, Sheng Y Q, Li C H, Zaho X F, Lu Z Y, Man B Y, Jiao Y and Jiang S Z 2018 *Appl. Surf. Sci.* **433** 45

[98] Kalanoor B S, Bisht P B, Akbar Ali S, Baby T T and Ramaprabhu S 2012 *J. Opt. Soc. Am. B* **29** 669

[99] Zheng C, Chen W Z, Huang Y Y, Xiao X Q and Ye X Y 2014 *RSC Adv.* **4** 39697

[100] Sadrolhosseini A R, Noor A S M, Faraji N, Kharazmi A and Mahdi M A 2014 *J. Nanomater* **2014** 962917

[101] Biswas S, Kole A K, Tiwary C S and Kumbhakar P 2016 *Rsc. Adv.* **6** 10319

[102] Ouyang Q Y, Xu Z, Lei Z Y, Dong H L, Qi L H, Li C Y and Chen Y J 2014 *Carbon* **67** 214

[103] Wu L F, Wang Y H, Li P L, Wu X, Shang M, Xiong Z Z, Zhang G J, Liang F, Xie Y F and Wang J 2018 *J. Alloys Compd.* **777** 759

[104] Zhang X L, Zhao X, Liu Z B, Shi S, Zhou W Y, Tian J G, Xu Y F and Chen Y S 2011 *J. Opt.* **13** 075202

[105] Darabi H, Adelifard M and Rajabi Y 2019 *J. Nonlinear Opt. Phys.* **28** 1950005

[106] Ouyang Q Y, Yu H L, Xu Z, Zhang Y, Li C Y, Qi L H and Chen Y J 2013 *Appl. Phys. Lett.* **102** 031912

[107] Feng M, Sun R Q, Zhan H B and Chen Y 2010 *Nanotechnology* **21** 75601

[108] Ouyang Q Y, Yu H L, Wu H Y, Lei Z Y, Qi L H and Chen Y J 2013 *Opt. Mater.* **35** 2352

[109] Ouyang Q Y, Di X P, Lei Z Y, Qi L H, Li C Y and Chen Y J 2013 *Phys. Chem. Chem. Phys.* **15** 11048

[110] Li P L, Wang Y H, Shang M, Wu L F and Yu X X 2020 *Carbon* **159** 1

[111] Li P C, Zhu B H, Li P, Zhang Z H, Li L Y and Gu Y Z 2019 *Nanomaterials* **9** 957

[112] Zhao M, Peng R, Zheng Q, Wang Q, Chang M J, Liu Y, Song Y L and Zhang H L 2015 *Nanoscale* **7** 9268

[113] Remyamol T, John H and Gopinath P 2013 *Carbon* **59** 308

[114] Zhang X Y, Liu Z B, Huang Y, Wan X J, Tian J G, Ma Y F and Chen Y S 2009 *J Nanosci. Nanotechnol.* **9** 5752

[115] Zhang X L, Zhao X, Liu Z B, Liu Y S, Chen Y S and Tian J G 2009 *Opt. Express* **17** 23959

[116] Bala Murali Krishna M, Venkatramaiah N, Venkatesan R and Narayana Rao D 2011 *Appl. Phys. Lett.* **98** 081106

[117] Wang A J, Long L L, Zhao W, Song Y L, Humphrey M G, Cifuentes M P, Wu X Z, Fu Y S, Zhang D D, Li X F and Zhang C 2013 *Carbon* **53** 327

[118] Husaini S, Lesko A, Heckman E M and Bedford R G 2014 *CLEO* **7**

[119] Al-Asadi A S, Hassan Q M A, Abdulkader A F, Mohammed M H, Bakr H and Emshary C A 2019 *Opt. Mater.* **89** 460

[120] Liao Y Z, Zhang C, Wang X, Li X G, Ippolito S J, Kalantar-zadeh K and Kaner R B 2011 *J. Phys. Chem. C* **115** 16187

[121] Sajan D, Vijayan N, Safakath K and Karabacak K 2013 *Spectrochim. Acta A* **108** 197

[122] Kamjou Mansour 1992 *J. Opt. Soc. Am. B* **9** 1100

[123] Laurent V, Didier R, Jean-François D, Jacques A D, François H and Eric A 2002 *J. Opt. Soc. Am. B* **19** 208